J. Chem. Sci., Vol. 122, No. 3, May 2010, pp. 381–389. © Indian Academy of Sciences.

A solid-polymer-electrolyte direct methanol fuel cell (DMFC) with Pt–Ru nanoparticles supported onto poly(3,4-ethylenedioxythiophene) and polystyrene sulphonic acid polymer composite as anode

K K TINTULA[a], S PITCHUMANI[a], P SRIDHAR[a] and A K SHUKLA[b,*]

[a]Central Electrochemical Research Institute (CSIR), Madras Unit, Chennai 600 113
[b]Solid State and Structural Chemistry Unit, Indian Institute of Science, Bangalore 560 012
e-mail: shukla@sscu.iisc.ernet.in

MS received 8 December 2009; revised 19 February 2010; accepted 23 February 2010

Abstract. Nano-sized Pt–Ru supported onto a mixed-conducting polymer composite comprising poly(3,4-ethylenedioxythiophene)-polystyrene sulphonic acid (PEDOT–PSSA) is employed as anode in a solid-polymer-electrolyte direct methanol fuel cell (SPE–DMFC) and its performance compared with the SPE–DMFC employing conventional Vulcan XC-72R carbon supported Pt–Ru anode. Physical characterization of the catalyst is conducted by Fourier-transform infra-red (FTIR) spectroscopy, X-ray diffraction (XRD), Scanning electron microscopy (SEM) and Energy dispersive X-ray analysis (EDAX) in conjunction with cyclic voltammetry and chronoamperometry. The study suggests that PEDOT–PSSA to be a promising alternative catalyst-support-material for SPE–DMFCs.

Keywords. Poly(3,4-ethylenedioxythiophene) and poly (styrene sulphonic acid); catalyst support; DMFC; corrosion.

1. Introduction

The direct use of methanol in a fuel cell clearly offers considerable attractions from the point of view of simplicity of design and hence, potentially, of cost.[1–3] In essence, a solid-polymer-electrolyte direct methanol fuel cell comprises an anode at which methanol is electrochemically oxidized to carbon-di-oxide, a cathode at which oxygen is reduced to water and a Nafion membrane that acts as electrolyte. One of the main drawbacks of the solid-polymer-electrolyte direct methanol fuel cells (SPE–DMFCs) is the sluggish anode reaction, which, coupled with the inefficient cathode reaction gives rise to low overall cell performance.[4–10]

As revealed in the literature, several efforts have been made to enhance the electro-oxidation of methanol by tailoring the carbon-supported Pt–Ru catalyst.[11,12] But the choice of a suitable carbon support still remains a factor as it affects the performance of supported catalyst through interactions between the catalyst and the support that modify the catalyst activity.[13–15] These interactions are particularly dependent on the nature of the functional groups on the support. For instance, it is found that carbons with lower concentration of acid-base groups[13] and carbons with sulfur- or nitrogen-based functionalities[15] ameliorate the catalytic activity. Consequently, considerable efforts have been expended on the optimization and development of new support material such as graphite nanofibres,[16] carbon nanotubes[17,18] and mesocarbon microbeads[19] in order to improve both the oxidation rate and electrode stability towards methanol electro-oxidation. These materials have high surface-area that facilitates uniform dispersion of catalyst and, since these are electronically more conductive than carbon, these have also attracted attention as alternate support materials for fuel cell catalysts.

Conducting polymers due to their high electronic conductivity (10^{-6}–10^{3} S/cm), high stability and high surface-area have found wide applications in sensors, electrochemical actuators, electromagnetic shielding, corrosion inhibitors, and polymeric batteries.[20–23] The most common conducting polymers, such as polyaniline (PAni), polypyrrole (PPy), polythiophene (PTh) and their derivatives, used as fuel-cell-catalyst supports are conjugated polymers

*For correspondence

with heteroatoms in the main chain.[24–30] These polymers are especially attractive since their electronic conductivity values are about one to two orders higher than the carbon particles.[31] Of the entire conducting polymers, poly (3,4-ethylenedioxythiophene) (PEDOT), modified PTh, appears to be the most adequate support for fuel–cell catalysts. PEDOT is known to be stable with its electronic conductivity values ranging between 1–100 S/cm based on the dopant used;[32] it can also be doped with ionically-conducting polymers, such as polystyrene sulphonic acid (PSSA), to make it mixed (electronic + ionic) conducting. Drillet *et al*[33] were the first to demonstrate PEDOT-supported Pt as the anode for DMFCs; these authors observed a striking change in the morphology after prolonged storing of PEDOT reaction-layer in air and reported ameliorated performance in relation to freshly-prepared PEDOT reaction-layer. Recently, Arbizzani *et al.*[34,35] have studied a passive DMFC with PEDOT–PSSA supported Pt–Ru as catalyst both for its anode and cathode more so to demonstrate mixed (electron + proton) conduction in PEDOT–PSSA supported Pt–Ru catalyst and have reported mass activity for PEDOT–PSSA supported Pt–Ru catalyst to be similar to Vulcan XC-72 supported Pt–Ru catalyst. By contrast, Patra *et al*[36] have reported higher electrochemical activity towards methanol oxidation with Pt dispersed on PEDOT in relation to carbon-supported Pt.

The present study is an attempt to resolve the aforesaid paradox. The study comprises a detailed investigation on the electro-catalytic behaviour of PEDOT–PSSA supported Pt–Ru towards methanol oxidation wherein a comparison of the performance data for DMFCs employing mixed-conducting-PEDOT–PSSA-supported Pt–Ru and carbon-supported Pt–Ru suggests the former to be superior.

2. Experimental

2.1 *Materials*

All the chemicals used were of analytical grade. Chloroplatinic acid and ruthenium trichloride were purchased from Alfa Aesar. (3,4-ethylenedioxythiophene) EDOT was procured from Aldrich. Sodium salt of polystyrenesulfonic acid, formaldehyde, ferric nitrate, and methanol were obtained from Acros Organics and were used as received. Vulcan XC 72R carbon was obtained from Cabot Corporation. Polytetrafluroethylene (PTFE) and 5 wt.% Nafion solution were procured from Dupont and were used as received. De-ionized water (18 MΩ cm) was used during the study.

2.2 *Synthesis of PEDOT–PSSA composite*

PEDOT–PSSA composite was synthesized using the procedure described elsewhere.[37] In brief, EDOT was polymerized by mixing an aqueous solution of NaPSS with required amount of EDOT monomer and stirred for 30 min. To the aforesaid admixture, an excess of $Fe(NO_3)_3 \cdot 9H_2O$ dissolved in minimum amount of water was added drop-wise under stirring at room temperature (~25°C). The dark-blue coloured suspension thus obtained was filtered, washed copiously with de-ionized water. The resultant composite was dried at 50°C under vacuum.

2.3 *Preparation of Pt–Ru nanoparticle on PEDOT–PSSA and on Vulcan XC-72R carbon*

For supporting 1 : 1 Pt–Ru on PEDOT–PSSA, about 0·4 g of PEDOT–PSSA was sonicated in an ultrasonic bath with water for 15 min to which the required amount of chloroplatinic acid and ruthenium chloride were added as precursors. The mixture was stirred at room temperature for 30 min and formaldehyde was added to it followed by refluxing for 1 h at 80°C. After cooling, it was washed with copious amount of water, filtered and dried at 50°C for 4 h. Similarly, 1 : 1 Pt–Ru on Vulcan XC-72R carbon was obtained; in brief, the mixture containing 0·4 g of Vulcan XC-72R carbon and catalyst precursor was stirred at room temperature followed by heating up to 80°C. Subsequently, the pH of the solution was adjusted to 8·5 using 0·5 M NaOH solution. About 2 ml of 37 wt.% formaldehyde was added to it and kept under stirring for 1 h. After cooling, it was washed with copious amount of water, filtered and dried at 50°C for 4 h.

2.4 *Physicochemical characterization*

Formation and doped states of PEDOT were confirmed by recording Fourier-transform infra-red spectra on a Thermo Nicolet (Model Nexus 670) spectrometer. X-ray powder diffraction (XRD) patterns for the catalysts were obtained on a Philips Pan Analytical X-ray Diffractometer. The supported

catalysts were also examined under Scanning Electron Microscope (SEM-Model JEOL JSM 5400). The atomic compositions of Pt–Ru particles supported on PEDOT–PSSA and Vulcan XC 72R were analysed by Energy Dispersive Analysis of X-rays (EDAX) available with the SEM instrument.

2.5 *Fabrication of membrane electrode assembly (MEA)*

15 wt.% teflonised Toray-TGP-H-120 carbon paper of 0·37 mm thickness was used as the backing layer. To prepare the gas-diffusion layer (GDL), Vulcan XC-72R was suspended in cyclohexane and agitated in an ultrasonic water bath for 30 min. To this solution, 15 wt.% poly (tetrafluroethene) (PTFE) suspension in 2 mL ammonia was added with continuous agitation to form a slurry that was coated onto the backing layer uniformly until required loading of 1·5 mg cm^{-2} carbon was attained. GDL thus obtained was sintered in an air oven at 350°C for 30 min. For anode reaction layer, Pt–Ru-impregnated PEDOT–PSSA and Vulcan XC 72R were dispersed in ethanol and ultrasonicated for 30 min followed by the addition of required amount of Nafion solution (5 wt.%) and the resultant slurry was ultrasonicated for 1 h. The slurry thus obtained was coated onto the anode GDL till 2 mg cm^{-2} of Pt–Ru loading was attained; similarly, all cathode GDLs were coated with 2 mg cm^{-2} Pt. A thin layer of 1 : 1 solution of 5 wt.% Nafion and isopropyl alcohol was applied onto the surface of the electrode and the membrane electrode assembly was obtained by sandwiching the pre-treated Nafion-117 membrane between the two electrodes followed by its hot-pressing at 130°C for 3 min at a pressure of 60 kg cm^{-2}.

2.6 *Preparation of the working electrode*

The glassy carbon (GC) disk with geometrical area 0·071 cm^2 was used as working-electrode substrate for electrochemical measurements. The electrode was polished to a mirror finish with 0·06 μm alumina followed by rinsing in double-distilled water in an ultrasonicator. To prepare the working electrode, slurries of 60 wt.% Pt–Ru/PEDOT–PSSA and 60 wt.% Pt–Ru/Vulcan XC 72R were prepared by taking 5mg of the catalyst in 1ml of deionized water along with 5 wt.% Nafion as a binder. 5 μl of the dispersion was pipetted out on the top of the GC and the electrode was dried at room temperature (~ 25°C) to yield a Pt–Ru loading of ~ 200 $\mu g/cm^2$.

2.7 *Electrochemical characterization*

Electrochemical measurements were carried out using a potentiostat (Autolab PGSTAT 30) with conventional three electrode cell comprising a GC working electrode, Pt foil as the counter electrode and saturated calomel electrode (SCE) as the reference electrode. Cyclic voltammetric (CV) studies were performed in a solution containing 2 M CH_3OH solution in 0·5 M H_2SO_4 at a scan rate of 50 mV s^{-1}. Prior to the measurements nitrogen gas was purged for nearly 30 min, and stable and reproducible voltammograms were recorded after cycling in the potential region between –0·25 V and 1 V (vs SCE) in 0·5 M H_2SO_4 solution at 25°C. Chronoamperometry tests were conducted using a three electrode cell in a solution containing 2 M CH_3OH solution in 0·5 M H_2SO_4 at 0·6 V (vs SCE) for 3600 s.

2.8 *Performance evaluation of DMFCs*

MEAs were performance evaluated in a 4 cm^2 fuel–cell with parallel and parallel serpentine flow-field machined on graphite plates (Schunk Kohlenstofftechnic) for anode and cathode, respectively. For single cell polarization experiment an aqueous solution of 2 M methanol was fed to the anode of the DMFC through a peristaltic pump at 5 ml min^{-1} and humidified oxygen was fed to the cathode using a mass-flow controller (Aalborg Instruments and Controls, US) at a constant flow rate of 50 ml min^{-1} at atmospheric pressure. After equilibration, the fuel cell was tested at 70°C by taking galvanostatic polarisation data using a LCN100-36 electronic load procured from Bitrode Corporation, US. For half-cell polarization studies a three-electrode configuration was used. Gaseous hydrogen was fed to the cathode which served as both counter and reference electrodes. These measurements were carried out using a steady-state galvanostatic measurement at a scan rate of 10 mA s^{-1}. After DMFC became stable, it was subjected to ac impedance measurements in the frequency range between 10 kHz and 0·1 Hz at sinusoidal-potential-signal amplitude of 10 mVs^{-1} by using an Autolab-PGSTAT 30 at an operating cell voltage of 0·4 V.

3. Results and discussion

3.1 *Physicochemical characterization*

FT–IR spectra for pristine PEDOT–PSSA composite and 60 wt.% Pt–Ru supported on PEDOT–PSSA composite are shown in figure 1(a) and (b), respectively. Absorption peaks at 1320 and 1520 cm^{-1} correspond to C–C or C=C stretching modes of thiophene ring, while C–S vibration modes are seen at 682 cm^{-1}, 830 cm^{-1} and 927 cm^{-1}, and peaks at 1086 cm^{-1}, 1132 cm^{-1} and 1200 cm^{-1} are assigned to stretching mode of ethylene dioxy (C–O–C) group.[38]

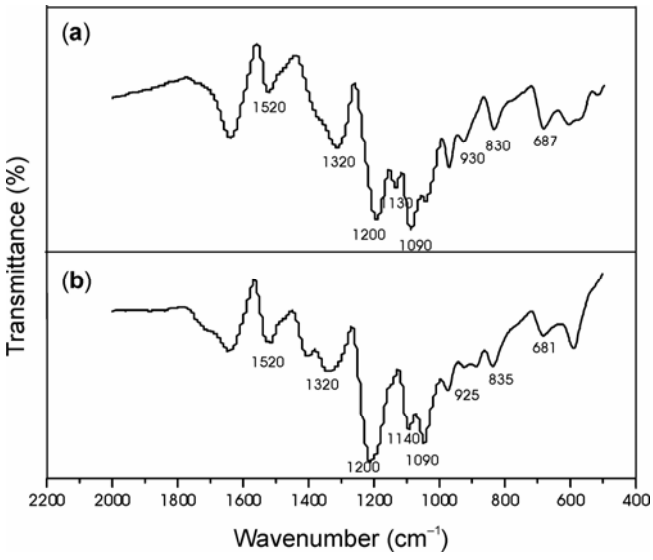

Figure 1. FTIR spectra for (**a**) PEDOT–PSSA powder and (**b**) (1 : 1) Pt–Ru/PEDOT–PSSA composite.

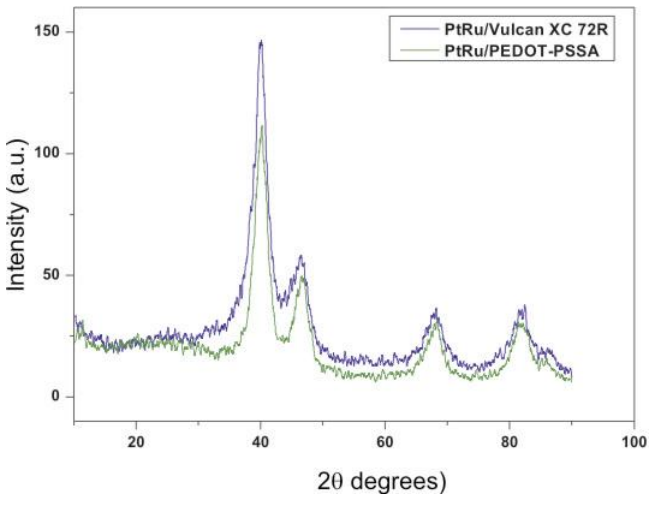

Figure 2. Powder X-ray diffraction patterns for Pt–Ru/PEDOT–PSSA and Pt–Ru/Vulcan XC 72R.

Both the spectra are nearly identical suggesting PEDOT structure was retained even after incorporating the catalyst. The presence of characteristic peaks at different vibration modes in the spectra confirms the formation of PEDOT.

Both the catalysts, namely Pt–Ru/Vulcan XC 72R and Pt–Ru/PEDOT–PSSA, are characterized by XRD. The powder X-ray diffraction patterns for the catalysts as shown in figure 2 exhibit diffraction peaks corresponding to (111), (200), (220), and (311) reflections akin to the face-centered-cubic (*fcc*) crystal structure for Pt. Incorporation of Ru into the *fcc* Pt structure is reflected by the shift in the diffraction peaks to higher values of 2θ.[39] Absence of characteristic reflections associated with a hexagonal close packed (*hcp*) structure of Ru implies formation of Pt–Ru structure. Differences appear only in the full-width at half maximum (FWHM) of the reflection peaks indicating a difference in the average particle sizes. The average particle sizes for the Pt–Ru particles supported onto PEDOT–PSSA and Vulcan XC 72R as evaluated by the Scherrer equation are 6 and 8 nm, respectively.

The electron micrographs for the catalysts are obtained using a SEM and their elemental composition determined by EDAX. The EDAX data for both Pt–Ru/PEDOT–PSSA and Pt–Ru/Vulcan XC 72R catalysts are shown in figure 3(a) and (b) along with their electron micrographs. The electron micrograph for Pt–Ru-dispersed onto PEDOT–PSSA shows a particulate morphology on the base polymer-matrix suitable for effective dispersion of Pt–Ru. Quantitative analysis by EDAX indicates Pt loadings of 36·4 wt.% and 37·2 wt.% and Ru loadings of 18·9 wt.% and 17·4 wt.% for Pt–Ru/PEDOT–PSSA and Pt–Ru/Vulcan XC-72, respectively, as against the desired loadings of 40 wt.% Pt and 20 wt.% Ru.

3.2 *Performance Evaluation of the catalysts towards methanol electro-oxidation*

Catalytic activity of Pt–Ru supported on PEDOT–PSSA is investigated towards electro-oxidation of methanol. Figure 4 shows cyclic voltammograms between –0·25 and 1·0 V (vs SCE) for the Pt–Ru/PEDOT–PSSA and Pt–Ru/Vulcan XC 72R catalysts in a solution containing 2 M CH_3OH in 0·5 M H_2SO_4. Changes in electrode reaction rates were estimated from the peak current density. In the voltammograms, the forward current peak (I_f) is attributed to the oxidation of methanol and the backward

peak is due to the oxidation of adsorbed intermediates. PEDOT–PSSA supported Pt–Ru exhibits a forward current peak of 10 mA cm^{-2} at 0·6 V (vs SCE) and shows higher methanol oxidation current in relation to carbon-supported Pt–Ru catalyst. This could be due to mixed-conducting nature of PEDOT–PSSA that enhances proton and electron transport within the anode catalyst, ameliorating the utilization of Pt–Ru catalyst.

In the literature,[40–42] it is reported that the long-term activity of Pt is due to the competitive adsorption of reaction intermediates on the surface of polyaniline. Accordingly, it is evident that the catalytic activity of electrocatalyst varies with the support. Cumulative effect of Ru and polymer matrix that adsorbs reaction intermediates makes Pt–Ru supported on PEDOT–PSSA tolerant to carbonaceous species accumulation. The mass activity (mA/mg $_{Pt–Ru}$) and I_f/I_b ratio for methanol oxidation at the respective peak-potentials are given in table 1. Although the I_f/I_b ratio is almost the same for both the catalysts, the improved mass activity for PtRu/PEDOT–PSSA elucidates ameliorated effect of PEDOT–PSSA higher efficiency over Vulcan XC72R. Superior wetting characteristics of PEDOT–PSSA composite in methanol may lead to higher utilization of the internal surface-area of the composite. Besides, the intrinsic proton conductivity of the composite allows methanol oxidation reaction to take place across the catalyst layer and reduces the number of phases for active reaction, which increases the active contact sites between the reactant and the catalyst. The presence of ionically-conducting PSSA in PEDOT may also improve the catalytic property of Pt–Ru in PEDOT–PSSA supported catalyst.

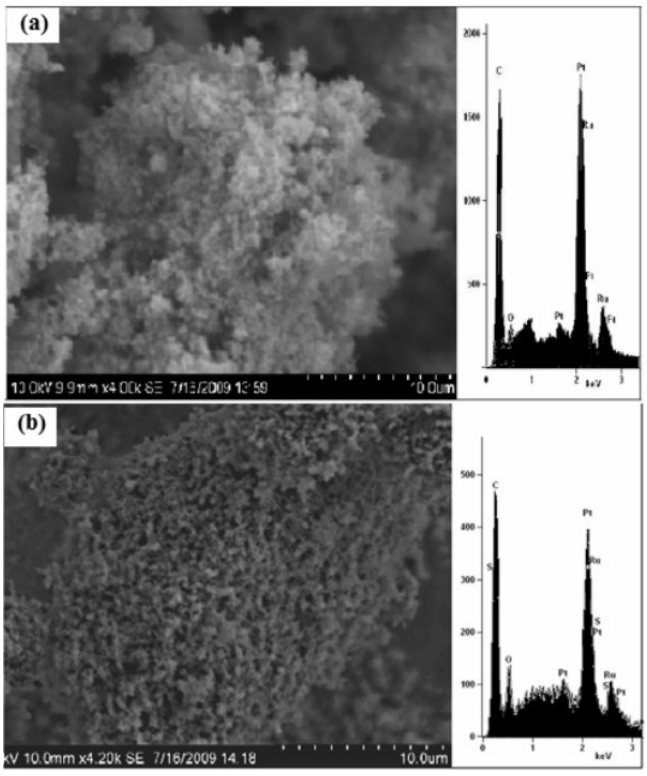

Figure 3. SEM images and EDAX spectra for (**a**) Pt–Ru/PEDOT–PSSA and (**b**) Pt/Vulcan XC 72R. The scale bar in both figures corresponds to 10 μm.

3.3 *Anode polarization*

To further evaluate the performance of Pt–Ru supported on PEDOT–PSSA and Vulcan XC 72R carbon towards methanol oxidation, DMFCs are assembled and anode polarization data are obtained

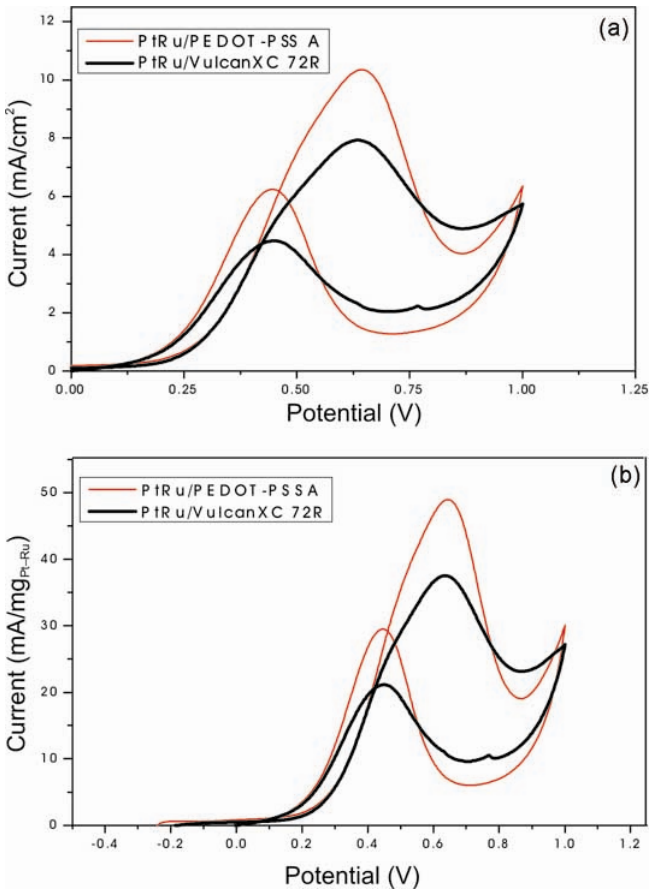

Figure 4. Cyclic voltammograms for methanol electrooxidation of Pt–Ru/PEDOT-PSSA and Pt–Ru/Vulcan XC 72R electrodes in 2 M methanol in 0·5 M H_2SO_4 solution at scan rate of 50 mV/s. (**a**) Normalized to area of the electrode. (**b**) Normalized to metal loading.

Table 1. Methanol oxidation data for Pt–Ru/PEDOT–PSSA and Pt–Ru/Vulcan XC 72R electrodes.

Catalyst	Mass activity (mA/mg of Pt–Ru)	Anodic peak potential (V)	I_f/I_b ratio	Activity ($A/mg_{Pt-Ru}/cm^2$)	Pt–Ru loading ($\mu g/cm^2$)
Pt–Ru/PEDOT–PSSA	48·97	0·638	1·8	0·689	210
Pt–Ru/Vulcan XC 72R	37·51	0·631	1·72	0·528	211

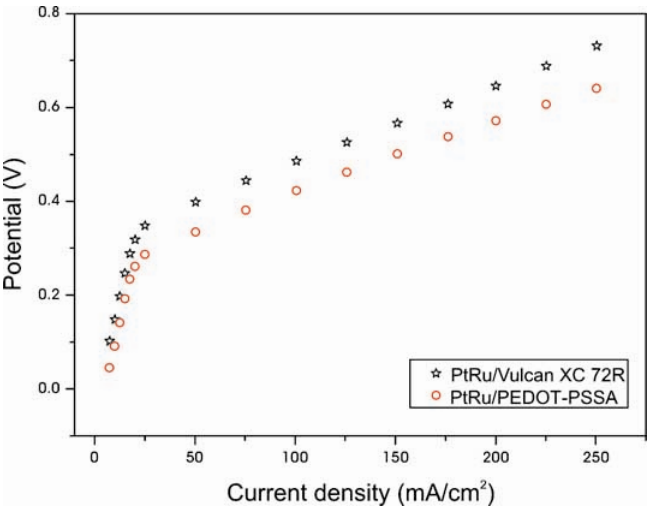

Figure 5. Anodic half-cell polarization behaviour of Pt–Ru/PEDOT- PSSA and Pt–Ru/Vulcan XC 72R at 70°C cell mode with 2M CH_3OH at anode at a flow rate of 1 ml min^{-1} and with N_2 streams at cathode (scan rate = 10 mV/s).

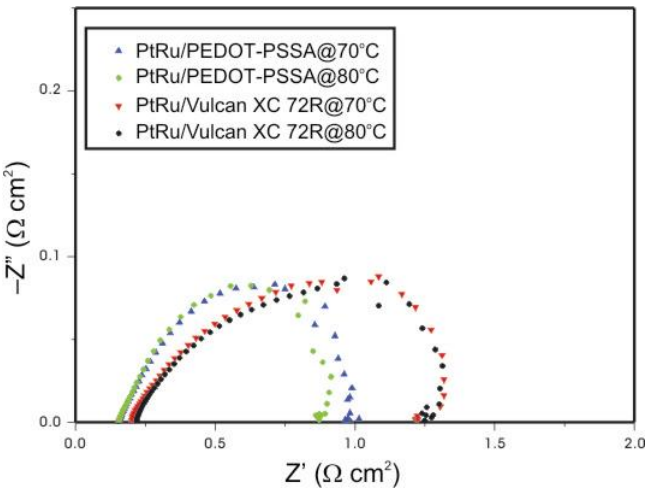

Figure 6. The Nyquist plot of DMFC assembled with Pt–Ru/PEDOT-PSSA and Pt–Ru/Vulcan XC 72R as anode material at 0.4V at various temperatures in cell mode with 2 M CH_3OH at anode at a flow rate of 1 ml min^{-1} and with O_2 streams at cathode.

as depicted in figure 5. The potential of Pt–Ru/PEDOT–PSSA anode is 0·5 V (vs DHE) at 150 mA cm^{-2}, which is about 65 mV lower in comparison with Pt–Ru/Vulcan XC 72R anode. This clearly indicates that PEDOT–PSSA supported Pt–Ru catalyst exhibits a higher catalytic activity for methanol oxidation.

3.4 *Impedance spectroscopy*

Impedance measurements (figure 6) are carried out at various temperatures and the results are interpreted by assuming an equivalent circuit as described by Seo and Lee.[43] To mitigate the influence of mass transport, impedance measurements are carried out at 0·4 V. It is observed that both ohmic and activation losses decrease as the cell temperature increases. The bulk (ionic + electronic) and contact resistances are observed at high frequencies. The diameter of the semicircle representing the charge-transfer resistance for PEDOT–PSSA and Vulcan XC 72R supported catalyst is about 0·80 Ω cm^2 and 1·08 Ω cm^2, respectively. The resistance of Pt–Ru/PEDOT–PSSA is lower in relation to Pt–Ru/Vulcan XC 72R as evident from the intercept of real impedance axis at low frequencies. It is presumed that the incorporation of PSSA into PEDOT increases the electronic resistance of the PEDOT–PSSA composite as also adds up to the proton conductivity that consequently decreases the total resistance of the system as suggested by Drillet *et al*.[33] The increase in proton conduction in the catalyst layer by PSSA-doped PEDOT creates a two-phase boundary necessary for electron and ion transfer as opposed to the three-phase boundary present when carbon is used as the support.[37]

3.5 *Chronoamperometry*

Chronoamperometric studies are conducted at 0·6 V (vs SCE) for electrodes with Pt–Ru/PEDOT–PSSA and Pt–Ru/Vulcan XC 72 R as the support material for about 3600 s to establish its stability towards methanol oxidation. To this end, working electrode, reference and counter electrodes are placed in a solution containing 2 M methanol in 0·5 M H_2SO_4.

From figure 7, it is seen that current degrades rapidly for 500 s, which could be due to the formation of intermediate species during methanol oxidation reaction.[44] Subsequently, the current response corresponding to Pt–Ru/PEDOT–PSSA stabilizes gradually unlike the case for Pt–Ru/Vulcan XC 72R. This characteristic of electrode makes them useful especially where fast start-up time or low equilibration times for DMFCs are desirable.

Corrosion current for both PEDOT–PSSA and Vulcan XC 72R are obtained under conditions stimulating carbon corrosion. The as-prepared electrodes were immersed in nitrogen purged 0·5 M sulphuric acid solution and current response as a function of time is measured at 0·9 V (vs Ag/AgCl). The chronoamperometric data (figure 8) shows lesser corrosion current for PEDOT–PSSA compared to Vulcan XC 72R for duration of 5 h. This suggests PEDOT–PSSA to be corrosion resistant and durable when used as a catalyst support.

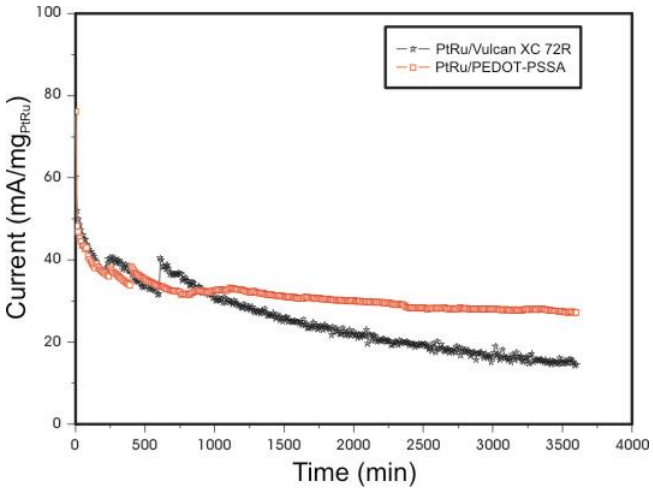

Figure 7. Chronoamperometric data for Pt–Ru/PEDOT-PSSA and Pt–Ru/Vulcan XC 72R at 0·6 V in 0·5 M H_2SO_4 consisting of 2 M methanol.

3.6 *Direct methanol fuel cell performance test*

The overall fuel–cell performance for the Pt–Ru nanoparticles supported on to PEDOT–PSSA and on to Vulcan XC 72R is compared in a practical DMFC. Figure 9 compares the performance of the DMFC anode comprising Pt–Ru/PEDOT–PSSA and Pt–Ru/Vulcan XC 72R nanocatalysts while using 2 M methanol at 70°C under similar test conditions. Table 2 displays the performance in $W/g_{Pt–Ru}$ with corresponding loading of the noble metals used in both anode and cathode. Anode comprising Pt–Ru supported PEDOT–PSSA shows higher open-circuit voltage and performance over the entire range of current density in relation to Pt–Ru supported on the Vulcan XC 72R. The DMFC with anode containing Pt–Ru/PEDOT–PSSA that yields a peak power density of 71 mW cm^{-2}, which is about 30% higher than the DMFC with anode containing Pt–Ru supported on the Vulcan XC 72R yields a peak power density of only 51 mW cm^{-2}. These data are consistent with the mass activity data obtained from the CV studies. It appears that further improvements in the conductivity of support and morphology of the Pt–

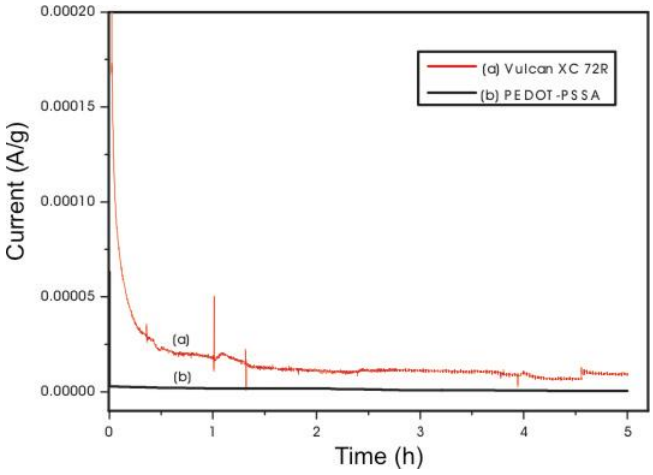

Figure 8. Chronoamperometric curve for Vulcan XC 72R and PEDOT–PSSA measured at 0·9 V in N_2 purged 0·5 M H_2SO_4.

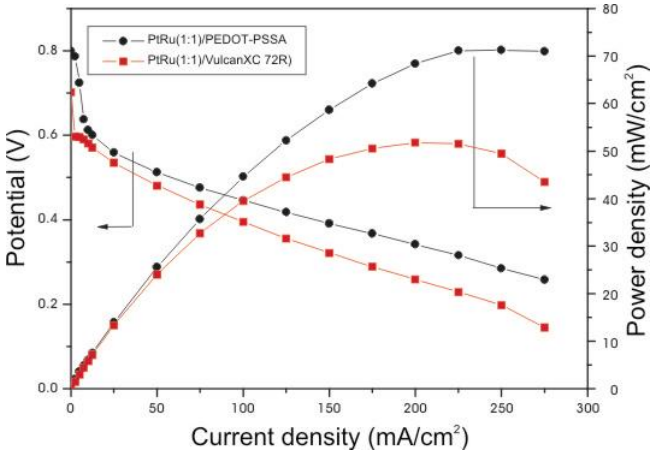

Figure 9. Comparison of DMFC performance using PEDOT–PSSA supported Pt–Ru and Vulcan XC 72R supported Pt–Ru catalysts at anode with 2 M methanol at 70°C.

Table 2. Current and P_{max} data for Pt–Ru/PEDOT–PSSA and Pt–Ru/Vulcan XC 72R electrodes employed in DMFC.

S. No	Anode support	Pt–Ru loading	Current (A g^{-1}_{Pt-Ru})	Power$_{max}$ (W g^{-1}_{Pt-Ru})
MEA 1	Pt–Ru/PEDOT–PSSA	2 mg/cm^2 (1·3 mg/cm^2 of Pt)	112·5	35·5
MEA 2	Pt–Ru/Vulcan XC 72R	2 mg/cm^2 (1·3 mg/cm^2 of Pt)	100	25·5

*Pt loading on cathode kept constant at 2mg/ cm^2 for both MEAs.

Ru/PEDOT–PSSA can help enhancing the cell performance.

4. Conclusions

The present study projects PEDOT–PSSA conducting-polymer composite as a promising support material for Pt–Ru and its ameliorating effect towards methanol-oxidation reaction. Electrochemical data demonstrate that Pt–Ru/PEDOT–PSSA has higher mass-activity than Pt–Ru/Vulcan XC72R. The ameliorating effect of the mixed-conducting PEDOT–PSSA composite is reflected by the improved performance of the DMFC and the related impedance measurements where the total system-resistance is found to be lower.

Acknowledgement

Financial support from the Council of Scientific and Industrial Research (CSIR), New Delhi under an EFYP supra-institutional project is gratefully acknowledged.

References

1. Larminie J and Dicks A 2003 *Fuel cell system explained* (New York: Wiley)
2. Scott K and Shukla A K 2007 *Modern aspects of electrochemistry* (Springer) pp 127–227
3. Ren X M, Zelenay P, Thomas A, Davey J and Gottesfeld S 2000 *J. Power Sources* **86** 111
4. Hampson N A, Willars M J and McNicol B D 1979 *J. Power Sources* **4** 191
5. Parsons R and VanderNoot T J 1988 *J. Electroanal. Chem* **9** 257
6. Iwasita-Vielstich T, Tobias C W and Gerischer H 1990 *Advances in electrochemical science and engineering* (Weinheim: VCH) vol. 1, p. 127
7. Cameron D S Hards G A and Thompsett D 1992 *Proc. Electrochem. Soc.* 10
8. Vielstich W and Iwasita T 1997 *Handbook of heterogeneous catalysis* (Chichester: Wiley) vol. 4
9. Kordesch K and Simader G 1996 *Fuel cells and their application* (Weinheim: VCH)
10. Selvarani G, Maheswari S, Sridhar P, Pitchumani S and Shukla A K 2009 *J. Electrochem. Soc.* **156** B1354
11. Liu H, Song C, Zhang L, Zhang J, Wang H and Wilkinson D P 2006 *J. Power Sources* **155** 95
12. Liu Z, Ling X Y, Su X and Lee J Y 2004 *J. Phys. Chem.* **B108** 8234
13. Uchida M, Aoyama Y, Tanabe N, Yanagihara N, Eda N and Ohta A 1995 *J. Electrochem. Soc.* **142** 2572
14. Aramata A, Kodera T and Masuda M 1988 *J. Appl. Electrochem.* **18** 577
15. Roy S C, Christensen P A, Hamnett A, Thomas K M and Trapp V 1996 *J. Electrochem. Soc.* **143** 3073
16. Liu Z L, Lin X H, Lee J Y, Zhang W, Han M and Gan L M 2002 *Langmuir* **18** 4054
17. Li W Z, Liang C H, Zhou W J, Qiu J S, Zhou Z H, Sun G Q and Xin Q, 2003 *J. Phys. Chem.* **B107** 6292
18. Prabhuram J, Zhao T S, Tang Z K, Chen R and Z X Liang 2006 *J. Phys. Chem.* **B110** 5245
19. Y C Liu, X P Qiu, Y Q Huang and W T Zhu 2002 *Carbon* **40** 2375
20. Salaneck W R, Clark D T and Samuelsen E J 1991 *Science and application of conducting polymers* (IOP Publishing)
21. Feast W J, Tsibouklis J, Pouwer K L, Groenendaal L and Meijer E W 1996 *Polymer* **37** 5017
22. Chiang J-C and MacDiarmid A G 1986 *Synt. Met.* **13** 193
23. Warren L F and Anderson D P 1987 *J. Electrochem. Soc.* **134** 101
24. Kitani A, Akashi T, Sugimoto K and Ito S 2001 *Synth. Met.* **121** 1301
25. Liu F J, Huang L M, Wen T C and Gopalan A 2007 *Synth. Met.* **157** 651
26. Kost K M, Bartak D E, Kazee B and Kuwana T 1988 *Anal. Chem.* **60** 2379
27. Rajesh B, Thampi K R, Bonard J M, Mathieu H J, Xanthopoulos N and Viswanathan B 2003 *Chem. Commun.* **16** 2033
28. Wu G, Li L, Li J H and Xu 2006 *J. Power Sources* **155** 118
29. Selvaraj V and Alagar M 2007 *Electrochem. Commun.* **9** 1145
30. Swathirajan S and Mikhali Y M 1992 *J. Electrochem. Soc.* **139** 2105
31. Qi Z and Pickup P G 1998 *Chem. Commun.* 2299
32. Yamato H, Ohwa M and Wernet W 1995 *J. Electroanal. Chem.* **397** 163
33. Drillet J-F, Dittmeyer R and JÜttner K 2007 *J. Appl. Electrochem.* **37** 1219

34. Arbizzani C, Biso M, Manferrari E and Mastragostino M 2008 *J. Power Sources* **178** 584
35. Arbizzani C, Biso M, Manferrari E and Mastragostino 2008 *J. Power Sources* **180** 41
36. Patra S and Munichandraiah N 2009 *Langmuir* **25** 1732
37. Lefebvre M C, Qi Z and Pickup P G 1999 *J. Electrochem. Soc.* **146** 2054
38. Yang Y, Jiang Y, Xu J and Yu J 2007 *Polymer* **48** 4459
39. Aricò A S, Creti P, Kim H, Mantegna R, Giordano N and Antonucci V 1996 *J. Electrochem. Soc.* **143** 5
40. Swathirajan S and Mikhail Y M 1992 *J. Electrochem. Soc.* **139** 2105
41. Bouzek K, Holzhauser P, Kodym R, Moravcova S and Paidar M 2007 *J. Appl. Electrochem.* **37** 137
42. Laborde H, Linger J-M and Lamy C 1994 *J. Appl. Electrochem.* **24** 219
43. Seo S H and Lee C S 2008 *Energy and Fuels* **22** 1204
44. Kabbabi A, Faure R, Durand R, Beden B, Hahn F, Leger J-M and Lamy C 1998 *J. Electroanal. Chem.* **41** 444